

Fig. 4 Viscous boundaries in central region by vapor screen technique; $\alpha = 7^\circ$; $x/L = 0.9$; $R_{\infty,x} = 9 \times 10^6$.

cation of maximum thickness of the viscous layer. This vortical motion induces a downward flow toward the centerline which then turns outward, drawing low energy fluid from the center area. The stagnating cross flow and the thinned boundary layer resulting from the departing fluid causes the increased heating to the centerline region. Highly thinned areas corresponding to the peak heating locations are observed in the central region on the sharp-apex delta and at symmetrically opposed locations off the centerline of the rounded apex delta. The relative magnitudes of the viscous-boundary height can be obtained from the scale provided, where the distance from the surface y has been normalized by the calculated laminar boundary-layer thickness¹⁰ (δ_{2-D}) over a two-dimensional plate at 7° incidence in a cold flow. The minimum normalized viscous thickness for the wings exhibiting high, localized heating is roughly 0.3, whereas the minimum for the hyperbola and parabola, which show low heating and shear in the same region, is about 0.7. The vapor screen at the $x/L = 0.9$ station (x = distance down centerline from apex) of the hyperbolic wing suggests the initiation of the thinned central region characteristic of the delta wing flow-field. Not shown is an upstream vapor screen at $x/L = 0.4$ on the hyperbolic wing, which reveals a nearly continuous viscous boundary across the span with only a slight depression at the center. Only at a station much closer to the apex was a similar result observed on the sharp-apex delta wing.

The present results show the feasibility of reducing the vortex-induced heating to the lee surface of slender wings by properly contouring the leading-edge planform. The possibility of reducing upper surface heating to other configurations, such as the space shuttle, by proper contouring of the apex region has yet to be explored. Since leeward heating peaks on a current shuttle configuration have been reported to be of the same magnitude as on the compression side at angle of attack,⁶ this problem deserves further study.

References

- 1 Whitehead, A. H., Jr., "Effects of Vortices on Delta Wing Lee-Side Heating at Mach 6," *AIAA Journal*, Vol. 8, No. 3, March 1970, pp. 599-600.
- 2 Whitehead, A. H., Jr., and Keyes, J. W., "Flow Phenomena and Separation Over Delta Wings with Trailing-Edge Flaps at Mach 6," *AIAA Journal*, Vol. 6, No. 12, Dec. 1968, pp. 2380-2387.

³ Bertram, M. H. and Henderson, A., Jr., "Some Recent Research with Viscous Interacting Flow in Hypersonic Streams," *Proceedings of Symposium on "Viscous Interaction Phenomena in Supersonic and Hypersonic Flow,"* HRL, ARL, Wright-Patterson Air Force Base, Ohio, May 7-8, 1969, Univ. of Dayton Press, Dayton, Ohio.

⁴ Maikapar, G. I., "Aerodynamic Heating of Lifting Bodies," AIAA Paper, Philadelphia, Pa., 1968.

⁵ Borovey, V. Ja. et. al., "Experimental Study of Heat Transfer on Lifting Body Surface in Supersonic Stream," *Heat Transfer 1970*, 4th International Heat Transfer Conference, Paris-Versailles, 1970.

⁶ Hefner, J. N. and Whitehead, A. H., Jr., "Lee Side Heating Investigations, Part I: Experimental Lee Side Heating Study of a Delta Wing Orbiter," NASA Space Shuttle Technology Conference, Hampton, Va., March 1971.

⁷ Moore, F. K., "Three-Dimensional Boundary Layer Theory," *Advances in Applied Mechanics*, Vol. IV, 1956, Academic Press, New York.

⁸ Jones, R. A. and Hunt, J. L., "Use of Fusible Temperature Indicators for Obtaining Quantitative Aerodynamic Heat-Transfer Data," TR R-230, Feb. 1966, NASA.

⁹ Cross, E. J., Jr. and Hankey, W. L., "Investigation of the Leeward Side of a Delta Wing at Hypersonic Speeds," *Journal of Spacecraft and Rockets*, Vol. 6, No. 2, Feb. 1969, pp. 185-190.

¹⁰ Bertram, M. H. and Feller, W. V., "A Simple Method for Determining Heat Transfer, Skin Friction, and Boundary-Layer Thickness for Hypersonic Laminar Boundary-Layer Flows in a Pressure Gradient," Memo 5-24-59L, June 1959, NASA.

Measurements of the Duration of Constant Reflected-Shock Temperature in a Reflected-Shock Tunnel

D. J. MONSON*

NASA Ames Research Center, Moffett Field, Calif.

MANY studies¹⁻⁴ have shown that for shock tunnels operated in the overtailored condition, the duration of constant temperature can be considerably less than the duration of constant pressure behind the reflected shock. Davies¹ postulated a mechanism for this shortening, due to bifurcation of the reflected shock resulting from its interaction with the wall boundary layer. This allows early penetration of driver gas to the end wall above a certain incident shock Mach number. Markstein⁵ applied a stability analysis to the problem and predicted breakdown of the contact surface and subsequent mixing of the driver and test gases above a certain Mach number.

In a recent series of chemical kinetic studies in a 6-in-diam, 43-ft-long shock tunnel using a cold helium driver and a test gas of 10% carbon dioxide, 40% nitrogen, and 50% helium, it was necessary to operate in the overtailored condition in order to achieve the required reflected-shock temperatures. In order to establish the duration of contamination-free test time, an attempt was made to measure the reflected-shock temperature in the tube by monitoring radiation from the infrared active CO₂ in the test gas ahead of the end wall. It was felt that if driver gas reached the end wall, the resulting dilution and cooling of the test gas would decrease the radiation. An alternative procedure is that of Bull and Edwards⁴ who added CO₂ to the driver gas and looked for the first indication of emission or absorption ahead of the end wall. Their data, however, indicated some erratic behavior, since with the CO₂ in the driver gas, dilution and cooling of the test gas have opposite effects on the radiation.

Received April 29, 1971.

* Research Scientist.

The present test setup consisted of an Indium Antimonide nitrogen-cooled I.R. detector looking across the shock tube through a sapphire port, one-inch upstream of the end wall. The detector looked through nearly one optical thickness of CO_2 for all test cases, at least before any significant boundary layer developed, so it initially saw radiation from all of the gas. Slit apertures limited the field of view up or downstream to a total angle of two degrees. Provisions were made to mount suitable filters to examine the desired radiation band. Side-wall pressures were measured at the same station by a Kistler piezoelectric pressure gage mounted in the tube wall. Other shock-tube instrumentation was standard.

CO_2 radiation bands centered at 4.3, 2.7, and 2.0 μ were evaluated for their suitability in indicating the reflected-shock temperature. Each band was in turn isolated using wide-band filters centered at the band centers. The 2.0 μ radiation band proved to be by far the most sensitive indicator of the changes that occurred within the test gas during a shot. Accordingly, the 2.0 μ band was chosen as the best possibility for looking at the test gas radiation.

Tests were made at four conditions between shock Mach numbers, M_s , of 2.6 and 3.5. These ranged from slightly above the computed tailoring Mach number of 2.2 to extremely overtailored. A typical side-wall pressure record showed a large jump resulting from the shock reflection at the end wall, followed by a further compression lasting a few milliseconds presumably resulting from successive shock reflections between the contact surface and the end wall, then a period of relatively constant pressure lasting several tens of milliseconds, and finally a sudden quenching of the pressure due to arrival of the rarefaction wave. As overtailoring increased, the percentage rise in pressure following the first shock reflection increased. A typical radiation trace exhibited the same behavior as the pressure trace, except that the radiation was in all cases quenched before arrival of the rarefaction wave. Near tailoring, the quenching of the radiation was moderate and gradual over the total time of the shot. For large overtailoring, the radiation was quenched very rapidly to a low level in a time short compared to the total test time.

The pressure and radiation test records were used to compute ideal and indicated reflected-shock temperature histories for the shots, and the results are shown in Fig. 1. The calculated ideal curves represent perfect gas temperatures computed using measured shock speeds and the usual shock relations to obtain the initial reflected-shock temperature.

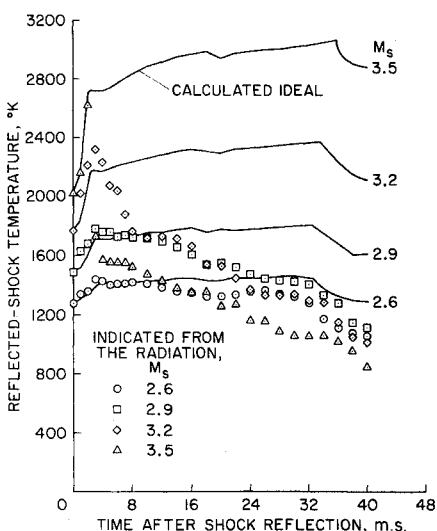


Fig. 1 Calculated ideal and indicated shock tube reflected shock temperature histories for a cold He driver gas and a 10% CO_2 , 40% N_2 , 50% He test gas.

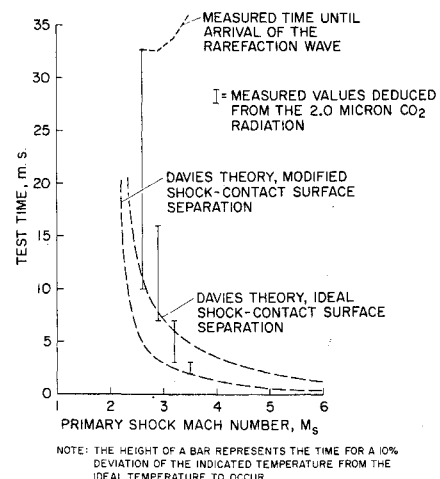


Fig. 2 Measured and calculated duration of contamination-free test gas at the end wall of a shock tube.

Subsequent ideal temperatures during a shot were computed using the measured pressure history together with the isentropic assumption. The indicated temperatures were computed by first assuming that the initial emission measured after the shock reflection at the end wall was from the test gas at the measured pressure and computed ideal temperature; subsequent indicated temperatures during a shot were computed by noting the changes in measured emission and pressure that occurred from the initial state and by using the CO_2 band emission charts of Echigo⁶ to obtain corresponding changes in indicated temperature. Note that at the lowest shock Mach number ($M_s = 2.6$) the two temperature calculations show excellent agreement for the first part of the shot; this is followed by a gradual drop in indicated temperature below the ideal temperature as the shot progresses. As the shock Mach number increases, an increasingly shorter period of agreement between the two temperatures is noted, and the indicated temperature deviates further from the ideal temperature. Indeed, above $M_s = 3.2$, there appears to be no time at all during the shot when the temperature could be considered to be relatively constant. This trend is consistent with previous measurements of the duration of constant reflected-shock temperatures in shock tubes operated in the overtailored condition.⁴

It is of interest to compare shock tube test times deduced from the present radiation measurements with the predictions of Davies theory for the times of first arrival of driver gas at the end wall due to shock bifurcation. These comparisons are presented in Fig. 2. For the measured values, the bottom of each bar is the time for the initial deviation of the indicated temperature from the ideal temperature for that test as shown in Fig. 1; the top of each bar represents the time for a 10% deviation to occur. The theoretical curves were calculated by Bull and Edwards⁴ using Davies theory for a gas mixture tailoring at $M_s = 2.2$, the same as the present case. Their results have been adjusted for the difference in shock tube lengths between the case they considered and the present tests. The two curves represent different assumptions about the location of the contact surface in the shock tube.⁴ Note that the measured test times corresponding to initial deviation of the indicated temperature from the ideal temperature, show good agreement with the predictions of Davies' theory. Also, as the tailoring Mach number is approached, less than 10% deviation of indicated temperature from the ideal temperature for the entire time of the shot is noted.

In conclusion, the present data are consistent with past studies which show that in shock tunnels operated in the overtailored condition, the duration of constant reflected-shock temperature can be considerably less than the duration

of constant reflected-shock pressure. The results show that monitoring the 2.0μ band radiation from small amounts of CO_2 in the test gas can be used to indicate usable test times in shock tunnels. Such indicated test times are in good agreement with the predictions of Davies' shock bifurcation model.

References

¹ Davies, L. and Wilson, J. L., "The Influence of Shock and Boundary Layer Interaction on Shock Tube Flows," A.R.C. 29 064-Hyp. 615, May 1967, National Physical Lab., Teddington, England.

² Lapworth, K. C., *The High Temperature Aspects of Hypersonic Flow*, AGARDograph 68, Pergamon, N.Y., 1964, pp. 255-267.

³ Richmond, J. K. and Parson, R. J., "Driver Gas Contamination in Shock Tunnels," D1-82-0806, Dec. 1968, Boeing Scientific Research Labs., Seattle, Wash.

⁴ Bull, D. C. and Edwards, D. H., "An Investigation of the Reflected Shock Interaction Process in a Shock Tube," *AIAA Journal*, Vol. 6, No. 8, Aug. 1968, pp. 1549-1555.

⁵ Markstein, G. H., "Flow Disturbances Induced Near a Slightly Wavy Contact Surface, or Flame Front, Traversed by a Shock Wave," *Journal of the Aerospace Sciences*, Vol. 238, No. 3 March 1958, pp. 238-239.

⁶ Echigo, R., "Evaluation of Band Emissivities of Carbon Dioxide and Water Vapour," *JSME Bulletin*, Vol. 10, Aug. 1967, pp. 671-679.

Mass Flow Rate Measurements in a Heterogeneous Medium

R. F. DAVEY*

California Institute of Technology, Pasadena, Calif.

Nomenclature

A, B	= calibration constants
d	= hot wire diameter
e	= voltage across hot wire
k	= thermal conductivity
L	= hot wire length
Nu	= Nusselt number = $e^2/r_w \pi L k \Delta T$
r_w	= hot wire resistance
Re	= Reynolds number = $\rho_f u d / \mu_f$
u	= gas velocity
ΔT	= hot wire overheat

Subscript

f	= value of parameter at the film temperature: $T_f = T + \frac{1}{2} \Delta T$
-----	--

1. Introduction

AN experimental study of the effect of a density gradient on the stability of a separated boundary layer led to the development of a new technique for measuring the mass flow rate in a nonuniform medium.¹ The small size of the experimental apparatus (the boundary-layer thickness was about 1 mm at the separation point) and the need to measure flow fluctuations made the sensor requirements particularly stringent. In fact, adequate spatial resolution and time response could be achieved only with a hot wire oriented spanwise to the two-dimensional flow.

Although hot wires have been used with great success for measuring the temperature and velocity of homogeneous flows, a single hot wire is, in general, unusable in a hetero-

Received April 28, 1971. This work was supported by the Office of Naval Research.

* Associate Research Engineer.

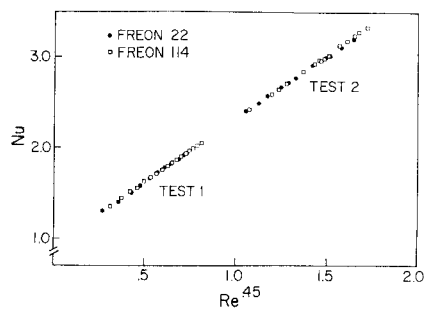


Fig. 1 Calibration of hot wires in Freon 22 and Freon 114.

geneous medium because the signal produced varies with changes in fluid properties (e.g., thermal conductivity, viscosity) as well as with changes in the flow parameters one wishes to measure. Following an analysis by Corrsin,² several investigators have used sensors with two or more hot wires, relying upon differences in overheat, length and wire diameter to obtain different sensitivities to composition and velocity. Although some success has been reported recently by Way and Libby³ using two wires and mixing the signals to obtain simultaneous velocity and density measurements, their probes require crossed sensors and, therefore, lack the spatial resolution required for the present application.

2. Analysis

The relationship governing the use of hot wires in fluid flows is King's law, usually expressed as: $Nu = A + B Re^n$. Collis and Williams⁴ gave a value of 0.45 for the power law exponent n in the range of Reynolds numbers used in the shear layer experiments. This value was verified by the calibration experiments discussed below.

If the hot wire equation is rewritten to represent a particular sensor operating at a fixed overheat, the overheat and all the parameters describing the hot wire can be included in the calibration constants, leaving

$$e^2 = A^*k + B^*(k/\mu_f^n)(\rho u)^n$$

It can be seen from this equation that if two gases could be found with equal thermal conductivities and viscosities, a single hot wire could be used to provide a measurement of mass flow rate in all mixtures of the gases. Since the shear layer experiments sought to determine the effect of a density gradient, a large difference in molecular weight was also desired. In general, these requirements are incompatible since the thermal conductivity usually decreases with increasing molecular weight. However, two Freons were found with a density ratio of 1.98 which nearly satisfied the requirements. Their properties are summarized in Table 1.

3. Experimental Evaluation

Several calibration experiments were performed to verify the theoretical predictions. In every case, measurements taken in the two Freons fell on a single calibration line, as predicted theoretically. The hot wires used were 90% platinum, 10% rhodium, with a diameter of 0.0001 in. and a length of 1 mm. They were heated using constant temperature bridge circuits to an overheat of about 300°C. This brought the resistance to 1.5 times the ambient temperature

Table 1 Properties of Freon 22 and Freon 114

Property	Freon 22	Freon 114	Ratio: 114/22
Molecular weight	86.48	170.93	1.976
k (joule/m-sec °K)	0.01172	0.01119	0.954
μ_f (poise)	1.59×10^{-4}	1.40×10^{-4}	0.881
$k/\mu_f^{0.45}$			0.991